International Journal of Engineering Science 94 (2015) 181–194

Contents lists available at ScienceDirect

International Journal of Engineering Science

journal homepage: www.elsevier.com/locate/ijengsci

Micromechanical investigations of polymer matrix composites with shape memory alloy reinforcement

Tian Tang *, Sergio D. Felicelli

Department of Mechanical Engineering, The University of Akron, Akron, OH 44325, United States

ARTICLE INFO

Article history:
Received 20 February 2015
Received in revised form 29 April 2015
Accepted 24 May 2015
Available online 19 June 2015

Keywords:
Shape memory alloys
Pseudoelastic behavior
Thermoviscoelastic matrix
Micromechanics
VAMUCH

ABSTRACT

In the present work, a micromechanics model was established to predict the effective time-dependent pseudoelastic responses of composites consisting of thermoviscoelastic polymer matrix and shape memory alloy (SMA) reinforcement. The incremental constitutive equations were firstly derived for polymer and SMA, respectively, and then formulated into a unified formulation. The starting point of the proposed model is to construct a variational statement which is a potential energy functional derived from the unified formulation. On account of the nonlinearity of the composites' behavior, the present model was developed based on an incremental procedure associated with the instantaneous effective tangential matrix of composites' coefficients. The present model offers an efficient tool for analyzing the SMA polymer matrix composites with arbitrary number and geometry of SMA reinforcement.

1. Introduction

Shape memory alloys (SMAs) are metallic alloys that are capable of recovering their original shape through the application of temperature or stress fields due to the phase transformation between austenitic and martensitic phases that SMAs undergo. Two main phenomena related to SMAs are: (i) The first one is pseudoelasticity (PE) in which very large nonlinear elastic strain can be generated especially upon loading, but full recovery is achieved in a hysteresis loop upon unloading; (ii) the second one is called shape memory effect (SME), which may be one-way or two-way. Due to these unique properties, SMAs are excellent candidates for sensors, large strain actuators, and other smart structures widely used in various areas of engineering fields such as aerospace, automotive, and biomechanical applications (Jani, Leary, Subic, & Gibson, 2014). During the past several decades, various numerical models have been developed in order to accurately describe the main behaviors of these alloys (Birman, 1997; Paiva & Savi, 2006). Generally speaking, these models are categorized into micro models (Warlimont, Delaey, Krishnan, & Tas, 1974; Nishiyama, 1978; Achenbach & Müller, 1982; Perkins, 1975) and macro phenomenological models (Paiva, Savi, Braga, & Pacheco, 2005; Brinson & Lammering, 1993; Brinson, 1993; Panico & Brinson, 2007; Lagoudas, BO, & Qidwai, 1996; Lagoudas, 2008).

SMA composites fabricated by embedding SMA fibers, particles, wires, or thin plates into metal matrix or polymer matrix have attracted great interest in the applications of a wide variety of smart materials and structures. Micromechanics models are indispensable tools to analyze the thermo-mechanical behavior of the SMA composite materials and structures. Boyd and Lagoudas (1994) employed Mori–Tanaka micromechanics model to predict the effective properties of polymer matrix

* Corresponding author. Tel.: +1 330 972 7672.
E-mail address: tiantang1991@gmail.com (T. Tang).

http://dx.doi.org/10.1016/j.ijengsci.2015.05.008
0020-7225/

composites with embedded SMA fibers, in which the polymer matrix was modeled as elastic materials. There are many other research works developed to understand the thermo-mechanical behavior of SMA composites with elastic matrix. For example, Damanpack, Aghdam, and Shakeri (2015) recently presented a finite element RVE (representative volume element) model to investigate the off-axis thermo-mechanical response of composites consisting of SMA and elastic polymeric matrix, in which the thermo-mechanical behavior of SMA was described using the constitutive model developed by Panico and Brinson (2007). Birman, Saravanos, and Hopkins (1996) and Saravanos, Birman, and Hopkins (1995) presented a combined micromechanics approach for the calculation of equivalent properties of the composite system consisting of SMA fibers within an elastic matrix in uniform thermal fields under longitudinal loads. They derived analytical solutions through the extension of Chamis's multi-cell micro-mechanics approach (Chamis, 1983) to predict the response of SMA composites with the assumption that the rate of transformation strain tensor is proportional to the rate of the martensite volumetric fraction. Gilat and Aboudi (2004) employed generalized method of cells (Aboudi, 1996) to analyze unidirectional composites with SMA fibers embedded in polymeric or metallic matrices subjected to thermal loadings. They adopted the 3D constitutive model of Lagoudas et al. (1996) to simulate the behavior of SMA. Furthermore, the polymeric matrix was assumed to be a linearly elastic material while the metallic matrix was modeled using the unified viscoplasticity theory of Bodner (2002). Based on the framework of HFGMC (Aboudi, 2004), Freed and Aboudi (2009) developed a micromechanics model to determine the effective mechanical properties and the two-way shape memory effect of SMA composites with SMA phase embedded in elastic resin matrix or elasto-viscoplastic matrix. Jarali, Raja, and Upadhya (2008) proposed an analytical micromechanical approach to evaluate the behavior of SMA composites consisting of SMA and elastic polymeric matrix under hygrothermal environment using the equivalent inclusion method proposed by Mura (1982).

The existing literatures show that numerous researchers have worked extensively to model the thermo-mechanical behavior of SMA composites with SMA reinforcements embedded in polymer or resin matrix. However, most of the research works considered the polymer or resin matrix as elastic materials. It is known that polymer or resin materials exhibit strong time-dependent viscoelastic behavior, which in turn causes the macroscopic viscoelastic response of SMA composites. Hence, it is absolutely needed that micromechanics models dealing with the time-dependent viscoelastic behavior of SMA composites with polymer or resin matrix are established for such purpose. In this study, based on the micromechanics framework VAMUCH (Yu & Tang, 2007), a micromechanics model was proposed to determine the time-dependent and nonlinear pseudoelastic behavior of SMA composites composed of SMA reinforcements and viscoelastic polymer matrix under thermo-mechanical loadings. The behavior of SMA phase was predicted using a 3D model extended from Brinson's one-dimensional model (Brinson & Lammering, 1993; Brinson, 1993), while the linear thermoviscoelastic behavior of the matrix was modeled by hereditary integral constitutive equation derived on the basis of Boltzmann superposition principle (Wineman & Rajagopal, 2000). Numerical examples were used to demonstrate the capability of the proposed model.

2. Incremental constitutive equations of materials

2.1. Incremental constitutive equations for linear thermo-viscoelastic polymer

Considering the linear thermo-viscoelastic polymer having no history of stress and deformation before time $t = 0$, then based on the Boltzmann superposition principle, the constitutive equations for the linear thermo-viscoelastic polymer can be expressed in the time domain in the following way,

$$\sigma_{ij}(t) = \int_0^t \left[C_{ijkl}(t-\tau)\dot{\varepsilon}(\tau) + \beta_{ij}(t-\tau)\dot{\theta}(\tau)\right]\mathrm{d}\tau \tag{1}$$

where $C_{ijkl}(t)$ is the stress relaxation stiffness tensor; $\dot{\varepsilon}_{kl}(\tau)$ is the strain rate; $\dot{\theta}(\tau)$ is the temperature change rate; $\sigma_{ij}(t)$ is the instantaneous stress tensor; $\beta_{ij}(t)$ is the instantaneous thermal stress tensor. Note that $\beta_{ij}(t) = -C_{ijkl}(t)\alpha_{kl}$ with α_{kl} being thermal expansion coefficients. In this study, the α_{kl} of the polymer are assumed to be constant.

According to the time–temperature superposition principle (Wineman & Rajagopal, 2000), the real time t have to be replaced with reduced time ξ in order to account for the variation of material's properties of polymer with temperature. Hence, the Eq. (1) can be rewritten as

$$\sigma_{ij}(t) = \int_0^t \left[C_{ijkl}(\xi-\xi')\dot{\varepsilon}_{kl}(\xi') + \beta_{ij}(\xi-\xi')\dot{\theta}(\xi')\right]\mathrm{d}\xi' \tag{2}$$

The reduced time $\xi = \xi(t)$ is defined by

$$\xi(t) = \int_0^t \frac{\mathrm{d}t'}{a_T} \tag{3}$$

where a_T is a time-scale shift factor, and $\xi' = \xi(\tau)$.

As pointed out by Pyatigorets, Marasteanu, Khazanovich, and Stolarski (2010), since the corresponding value of real time t can be found for each value of reduced time ξ and vice versa, the stress and strain in the reduced time domain can be replaced with their values found for the corresponding real time, such that

$$\sigma_{ij}(\xi) \equiv \sigma_{ij}(\xi(t)) \equiv \sigma_{ij}(t), \quad \varepsilon_{ij}(\xi) \equiv \varepsilon_{ij}(\xi(t)) \equiv \varepsilon_{ij}(t) \tag{4}$$

Hence, the Eq. (2) can be simplified as

$$\sigma_{ij}(t) = \int_0^t \left[C_{ijkl}(\xi(t) - \xi(\tau))\dot{\varepsilon}_{kl}(\tau) + \beta_{ij}(\xi(t) - \xi(\tau))\dot{\theta}(\tau)\right]\mathrm{d}\tau \tag{5}$$

In light of the nonlinear, time dependent, and multiphysics response of the composites, our analysis need to be incremental. The incremental formulations of Eq. (5) can be expressed as

$$\begin{aligned}\Delta\sigma_{ij}(t) &= \sigma_{ij}(t+\Delta t) - \sigma_{ij}(t)\\ &= \int_t^{t+\Delta t}\left[C_{ijkl}(\xi(t+\Delta t) - \xi(\tau))\dot{\varepsilon}_{kl}(\tau) + \beta_{ij}(\xi(t+\Delta t) - \xi(\tau))\dot{\theta}(\tau)\right]\mathrm{d}\tau\\ &\quad + \int_0^t\left[C_{ijkl}(\xi(t+t) - \xi(\tau))\dot{\varepsilon}_{kl}(\tau) + \beta_{ij}(\xi(t+t) - \xi(\tau))\dot{\theta}(\tau)\right]\mathrm{d}\tau\\ &\quad - \int_0^t\left[C_{ijkl}(\xi(t) - \xi(\tau))\dot{\varepsilon}_{kl}(\tau) + \beta_{ij}(\xi(t) - \xi(\tau))\dot{\theta}(\tau)\right]\mathrm{d}\tau\end{aligned} \tag{6}$$

Although the strain rate and temperature change rate are not necessarily constant in the whole time domain, it is reasonable to assume that the strain rate and temperature change rate are kept constant during each time increment Δt. Furthermore, the temperature change rate are assumed to be uniform in the whole composites. Then, the Eq. (6) can be rephrased as

$$\Delta\sigma_{ij}(t) = L_{ijkl}(t)\Delta\varepsilon_{kl}(t) + \gamma_{ij}(t)\Delta\theta(t) + \omega_{ij}(t) \tag{7}$$

where

$$\begin{aligned}L_{ijkl}(t) &= \frac{1}{\Delta t}\int_t^{t+\Delta t} C_{ijkl}[\xi(t+\Delta t) - \xi(\tau)]\mathrm{d}\tau\\ \gamma_{ij}(t) &= \frac{1}{\Delta t}\left(\int_t^{t+\Delta t}\beta_{ij}[\xi(t+\Delta t) - \xi(\tau)]\,\mathrm{d}\tau\right)\\ \omega_{ij}(t) &= \int_0^t\left[C_{ijkl}(\xi(t+\Delta t) - \xi(\tau)) - C_{ijkl}(\xi(t) - \xi(\tau))\right]\dot{\varepsilon}_{kl}(\tau)\mathrm{d}\tau + \int_0^t\left[\beta_{ij}(\xi(t+\Delta t) - \xi(\tau)) - \beta_{ij}(\xi(t) - \xi(\tau))\right]\dot{\theta}(\tau)\mathrm{d}\tau\end{aligned}$$

2.2. Incremental constitutive equations for shape memory alloys

Based on the one dimensional model of Brinson (Brinson & Lammering, 1993; Brinson, 1993), the three dimensional incremental thermo-mechanical constitutive equations of SMA might be expressed as

$$\Delta\sigma_{ij} = B_{ijkl}(\Psi)\Delta\varepsilon_{kl} + \beta_{ij}(\Psi)\Delta\theta + \Lambda_{ij}(\Psi)\Delta\Psi \tag{8}$$

where Ψ is an internal state variable representing the volume fraction of martensite. The elastic stiffness tensor of SMA, $B_{ijkl}(\Psi)$, is a function of the martensite fraction where the elastic moduli of SMA, $E(\Psi)$, is given by $E(\Psi) = E_A + \Psi(E_M - E_A)$ with E_M and E_A being the elastic moduli of pure martensite and austenite, respectively. $\beta_{ij}(\Psi)$ is the thermal stress tensor of the SMA and given by $\beta_{ij}(\Psi) = -B_{ijkl}(\Psi)\alpha_{kl}(\Psi)$ with $\alpha_{kl}(\Psi)$ being the thermal expansion coefficients of SMA, where $\alpha_{kl}(\Psi)$ is given by a linear combination such that $\alpha_{kl}(\Psi) = \alpha_{kl}^A + \Psi(\alpha_{kl}^M - \alpha_{kl}^A)$, where α_{kl}^A and α_{kl}^M are thermal expansion coefficients of pure austenite and martensite, respectively. The relationship between the transformation function $\Lambda_{ij}(\Psi)$ and elastic stiffness tensor of SMA is given by

$$\Lambda_{ij}(\Psi) = -B_{ijkl}(\Psi)(\varepsilon^L\delta_{kl}) \tag{9}$$

where δ_{kl} is Kronecker delta; ε^L is the maximum residual strain, which is assumed to be a constant material function.

The martensitic volume fraction Ψ is the summation of two distinct martensitic fractions in such a way that $\Psi = \Psi_s + \Psi_T$ with Ψ_s being the stress-induced martensite fraction, and Ψ_T being the temperature-induced martensite fraction.

The martensitic transformation evolution can be expressed by

(i) For $T > M_s$ and $\sigma_s^{Crit} + C_M(T - M_s) < \sigma^e < \sigma_f^{Crit} + C_M(T - M_s)$

$$\Psi_s = \frac{1 - \Psi_{s0}}{2}\cos\left\{\frac{\pi}{\sigma_s^{Crit} - \sigma_f^{Crit}}\left[\sigma^e - \sigma_f^{Crit} - C_M(T - M_s)\right]\right\} + \frac{1 + \Psi_{s0}}{2} \tag{10a}$$

$$\Psi_T = \Psi_{T0} - \frac{\Psi_{T0}}{1 - \Psi_{s0}}(\Psi_s - \Psi_{s0}) \tag{10b}$$

(ii) For $T < M_s$ and $\sigma_s^{Crit} < \sigma^e < \sigma_f^{Crit}$

$$\Psi_s = \frac{1-\Psi_{s0}}{2}\cos\left[\frac{\pi}{\sigma_s^{Crit}-\sigma_f^{Crit}}\left(\sigma^e-\sigma_f^{Crit}\right)\right]+\frac{1+\Psi_{s0}}{2} \tag{11a}$$

$$\Psi_T = \Psi_{T0}-\frac{\Psi_{T0}}{1-\Psi_{s0}}(\Psi_s-\Psi_{s0})+\Delta\varphi \tag{11b}$$

where

$$\Delta\varphi = \begin{cases} \frac{1-\Psi_{s0}}{2}\left\{\cos\left[a_M(T-M_f)\right]+1\right\} & \text{if } M_f < T < M_s,\ T < T_0 \\ 0 & \text{else} \end{cases} \tag{12}$$

The reverse transformation to austenite holds for $C_A(T-A_f) < \sigma^e < C_A(T-A_s)$ and $T > A_s$, and is expressed as

$$\Psi_s = \frac{\Psi_{s0}}{2}\left\{\cos\left[a_A\left(T-A_s-\frac{\sigma^e}{C_A}\right)\right]+1\right\} \tag{13a}$$

$$\Psi_T = \frac{\Psi_{T0}}{2}\left\{\cos\left[a_A\left(T-A_s-\frac{\sigma^e}{C_A}\right)\right]+1\right\} \tag{13b}$$

where the parameters a_M and a_A are defined as

$$a_M = \frac{\pi}{M_s-M_f} \quad a_A = \frac{\pi}{A_f-A_s} \tag{14}$$

Other parameters in Eqs. (10–13) include the four important temperature parameters: martensite finish temperature, M_f, martensite start temperature, M_s, austenite start temperature, A_s, and austenite finish temperature, A_f. The constants C_M and C_A are material properties represent the relationship between the temperature and critical transformation stress. σ_s^{Crit} and σ_f^{Crit} are critical transformation stress at both start and finish of transformation, respectively. σ^e is von Mises stress. Ψ_{s0} and Ψ_{T0} are the volume fractions of the stress induced and temperature induced martensite immediately before the transformation starts, respectively.

Finally, the increment of martensitic volume fraction can be obtained as

$$\Delta\Psi = \frac{\partial\Psi}{\partial T}\Delta T+\frac{\partial\Psi}{\partial\sigma^e}\Delta\sigma^e \tag{15}$$

3. Micromechanics model

Consider the smart composites with periodic microstructure as shown in Fig. 1. Two coordinate systems $x = (x_1, x_2, x_3)$ and $y = (y_1, y_2, y_3)$ are adopted to facilitate the micromechanics formulations. We use x_i as the global coordinates to describe the macroscopic structure and y_i parallel to x_i as the local coordinates to describe the unit cell (UC) (Here and throughout the

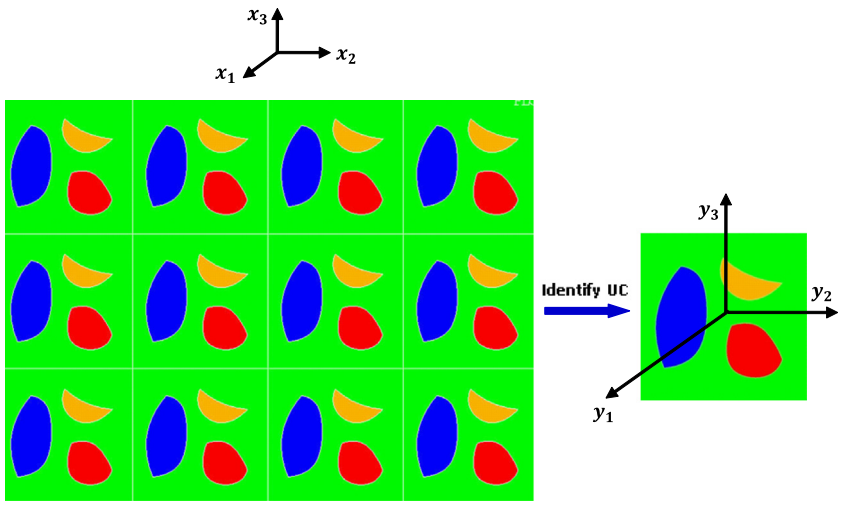

Fig. 1. A sketch of periodic heterogeneous materials (only two-dimensional (2D) UC is drawn for clarity).

paper, Latin indices assume 1, 2, and 3 and repeated indices are summed over their range except where explicitly indicated). We choose the origin of the local coordinate system y_i to be the geometric center of the UC.

3.1. Unified incremental constitutive equations for composite and its constituents

The unified incremental formulations of the locally nonlinear and time-dependent mechanical responses of the constituents of the composites consisting of SMA and polymer matrix might be expressed as

$$\Delta\sigma_{ij}(t,\Psi) = M_{ijkl}(t,\Psi)\Delta\varepsilon_{kl}(t) + \eta_{ij}(t,\Psi)\Delta\theta(t) + \varpi_{ij}(t,\Psi) \tag{16}$$

where

$$M_{ijkl}(t,\Psi) = \begin{cases} L_{ijkl}(t) & \text{for polymer materials} \\ B_{ijkl}(\Psi) & \text{for SMA} \end{cases}$$

$$\eta_{ij}(t,\Psi) = \begin{cases} \gamma_{ij}(t) & \text{for polymer materials} \\ \beta_{ij}(\Psi) & \text{for SMA} \end{cases}$$

$$\varpi_{ij}(t,\Psi) = \begin{cases} \omega_{ij}(t) & \text{for polymer materials} \\ \Lambda_{ij}(\Psi)\Delta\Psi & \text{for SMA} \end{cases}$$

Eq. (16) can be derived by

$$\Delta\sigma_{ij}(t) = \frac{\partial[\Delta U(t,\Psi)]}{\partial[\Delta\varepsilon_{ij}(t)]} \tag{17}$$

where the instantaneous energy increment $\Delta U(t,\Psi)$ is given by

$$\Delta U(t,\Psi) = \frac{1}{2}M_{ijkl}(t,\Psi)\Delta\varepsilon_{ij}(t)\Delta\varepsilon_{kl}(t) + \eta_{ij}(t,\Psi)\Delta\varepsilon_{ij}(t)\Delta\theta(t) + \varpi_{ij}(t,\Psi)\Delta\varepsilon_{ij}(t) + \frac{1}{2}G\Delta\theta(t) + \frac{1}{2}c_v\frac{\Delta\theta(t)^2}{T_0} + \frac{1}{2}h_v \tag{18}$$

where G is the energy change per unit temperature; c_v is the specific heat per unit volume at constant volume; T_0 is the reference temperature at which the constituent material is stress free; h_v, which is the energy change similar to c_v, represents the ratio of the energy added or removed from materials to the resulting martensite's volume fraction change.

The effective instantaneous properties of the SMA composite materials can be defined in the following two ways

$$\Delta\bar{\sigma}_{ij}(t,\Psi) = M^*_{ijkl}(t,\Psi)\Delta\bar{\varepsilon}_{kl}(t) + \eta^*_{ij}(t,\Psi)\Delta\theta(t) + \varpi^*_{ij}(t,\Psi) \tag{19}$$

$$\frac{1}{\Omega}\int_\Omega\left[\frac{1}{2}M_{ijkl}(t,\Psi)\Delta\varepsilon_{ij}(t)\Delta\varepsilon_{kl}(t) + \eta_{ij}(t,\Psi)\Delta\varepsilon_{ij}(t)\Delta\theta(t) + \varpi_{ij}(t,\Psi)\Delta\varepsilon_{ij}(t) + \frac{1}{2}G\Delta\theta(t) + \frac{1}{2}c_v\frac{\Delta\theta(t)^2}{T_0} + \frac{1}{2}h_v\right]$$
$$\mathrm{d}\Omega = \frac{1}{2}M^*_{ijkl}(t,\Psi)\Delta\bar{\varepsilon}_{ij}(t)\Delta\bar{\varepsilon}_{kl}(t) + \eta^*_{ij}(t,\Psi)\Delta\bar{\varepsilon}_{ij}(t)\Delta\theta(t) + \varpi^*_{ij}(t,\Psi)\Delta\bar{\varepsilon}_{ij}(t) + \frac{1}{2}G^*\Delta\theta(t) + \frac{1}{2}c^*_v\frac{\Delta\theta(t)^2}{T_0} + \frac{1}{2}h^*_v \tag{20}$$

where $\Delta\bar{\varepsilon}_{ij}$ are the increments of the global strain tensor; Superscripts "$*$" denote the effective properties whose calculations are determined by the micromechanics model; Ω is the volume of unit cell.

3.2. VAMUCH model

Starting from free energy in Eq. (18) and following the identical derivation procedure described in (Yu & Tang, 2007; Tang & Felicelli, 2015), we can finally formulate the variational statement, which govern the micromechanics model, as minimizing the following functional

$$\Pi_\Omega = \frac{1}{\Omega}\int_\Omega\left\{\frac{1}{2}M_{ijkl}(t,\Psi)\left[\Delta\bar{\varepsilon}_{ij} + \chi_{(i|j)}\right]\left[\bar{\varepsilon}_{kl} + \chi_{(k|l)}\right] + \eta_{ij}(t,\Psi)\left[\bar{\varepsilon}_{ij} + \chi_{(i|j)}\right]\Delta\theta(t) + \varpi_{ij}(t,\Psi)\left[\bar{\varepsilon}_{ij} + \chi_{(i|j)}\right]\right.$$
$$\left. + \frac{1}{2}G\Delta\theta(t) + \frac{1}{2}c_v\frac{\Delta\theta(t)^2}{T_0} + \frac{1}{2}h_v\right\}\mathrm{d}\Omega \tag{21}$$

under the following periodic constraints

$$\chi_i^{+j} = \chi_i^{-j} \quad \text{for } i, j = 1, 2, 3 \tag{22}$$

with $\chi_i^{+j} = \chi_i|_{y_j = d_j/2}$ and $\chi_i^{-j} = \chi_i|_{y_j = -d_j/2}$. Here, χ_i is the commonly called fluctuating function and d_j is the size of unit cell. Since $\Delta\varepsilon_{ij}(t) = \Delta\bar{\varepsilon}_{ij} + \chi_{(i|j)}$, we introduced the following matrix notations:

$$\Delta\bar{\epsilon}(t) = \lfloor \Delta\bar{\varepsilon}_{11}(t)\ 2\Delta\bar{\varepsilon}_{12}(t)\Delta\bar{\varepsilon}_{22}(t)\ 2\Delta\bar{\varepsilon}_{13}(t)\ 2\Delta\bar{\varepsilon}_{23}(t)\ \Delta\bar{\varepsilon}_{33}(t)\rfloor^T \tag{23a}$$

$$\Delta\epsilon_1 = \lfloor \Delta\hat{\varepsilon}_{11}(t)\ 2\Delta\hat{\varepsilon}_{12}(t)\ \Delta\hat{\varepsilon}_{22}(t)\ 2\Delta\hat{\varepsilon}_{13}(t)\ 2\Delta\hat{\varepsilon}_{23}(t)\ \Delta\hat{\varepsilon}_{33}(t)\rfloor^T \tag{23b}$$

where

$$\Delta\bar{\varepsilon}_{ij}(t) = \frac{1}{2}\left[\frac{\partial \Delta v_i(t;\boldsymbol{x})}{\partial x_j} + \frac{\partial \Delta v_j(t;\boldsymbol{x})}{\partial x_i}\right] \tag{24a}$$

$$\Delta\hat{\varepsilon}_{ij}(t) = \chi_{(i|j)} = \frac{1}{2}\left[\frac{\partial \chi_i(t;\boldsymbol{x};\boldsymbol{y})}{\partial y_j} + \frac{\partial \chi_j(t;\boldsymbol{x};\boldsymbol{y})}{\partial y_i}\right] \tag{24b}$$

where $\Delta v_i(t;\boldsymbol{x}) = \frac{1}{\Omega}\int_\Omega [\Delta u_i(t;\boldsymbol{x};\boldsymbol{y})]\,\mathrm{d}\Omega$ with $\Delta u_i(t;x;y)$ being the local increments of displacement vectors that is expressed as: $\Delta u_i(t;\boldsymbol{x};\boldsymbol{y}) = \Delta v_i(t;\boldsymbol{x}) + y_j\frac{\partial \Delta v_i}{\partial x_j} + \chi_i(t;\boldsymbol{x};\boldsymbol{y})$.

The matrix form of $\Delta\epsilon_1$ in Eq. (23b) is given by

$$\Delta\epsilon_1 = \begin{bmatrix} \frac{\partial}{\partial y_1} & 0 & 0 \\ \frac{\partial}{\partial y_2} & \frac{\partial}{\partial y_1} & 0 \\ 0 & \frac{\partial}{\partial y_2} & 0 \\ \frac{\partial}{\partial y_3} & 0 & \frac{\partial}{\partial y_1} \\ 0 & \frac{\partial}{\partial y_2} & \frac{\partial}{\partial y_3} \\ 0 & 0 & \frac{\partial}{\partial y_3} \end{bmatrix} \begin{Bmatrix} \chi_1 \\ \chi_2 \\ \chi_3 \end{Bmatrix} \equiv \Gamma_h\chi \tag{25}$$

where Γ_h is an operator matrix and χ is a column matrix containing the three components of the fluctuation functions. We discretize χ using finite elements as

$$\chi(x_i;y_i) = S(y_i)\boldsymbol{X}(x_i) \tag{26}$$

where S represents the shape function (in assemble sense excluding the constrained node and slave nodes) and $\boldsymbol{X}$ is the column matrix of the nodal value of the fluctuation functions for all active nodes. Substituting Eqs. (23–26) into Eq. (21), we obtain a discretized version of the functional as

$$\begin{aligned}\Pi_\Omega = \frac{1}{2\Omega}\Big(&\boldsymbol{X}^T E\boldsymbol{X} + 2\boldsymbol{X}^T D_{h\varepsilon}\Delta\bar{\epsilon}(t) + \left[\Delta\bar{\epsilon}_{(}t)\right]^T D_{\varepsilon\varepsilon}\Delta\bar{\epsilon}(t) + 2\boldsymbol{X}^T D_{h\theta}\Delta\theta(t) + 2[\Delta\bar{\epsilon}(t)]^T D_{\varepsilon\theta}\Delta\theta(t) + 2\boldsymbol{X}^T D_{hc} \\ &+ 2[\Delta\bar{\epsilon}(t)]^T D_{\varepsilon C} + D_{\psi\psi}\Delta\theta(t) + D_{\theta\theta}\frac{\Delta\theta(t)^2}{T_0} + D_{CC}\Big)\end{aligned} \tag{27}$$

where

$$\begin{aligned} E &= \textstyle\int_\Omega (\Gamma_h S)^T M(\Gamma_h S)\,\mathrm{d}\Omega & D_{h\varepsilon} &= \textstyle\int_\Omega (\Gamma_h S)^T M\,\mathrm{d}\Omega \\ D_{\varepsilon\varepsilon} &= \textstyle\int_\Omega M\,\mathrm{d}\Omega & D_{h\theta} &= \textstyle\int_\Omega (\Gamma_h S)^T \eta\,\mathrm{d}\Omega \\ D_{\varepsilon\theta} &= \textstyle\int_\Omega \eta\,\mathrm{d}\Omega & D_{hC} &= \textstyle\int_\Omega (\Gamma_h S)^T \varpi\,\mathrm{d}\Omega \\ D_{\varepsilon C} &= \textstyle\int_\Omega \varpi\,\mathrm{d}\Omega & D_{\psi\psi} &= \textstyle\int_\Omega G\,\mathrm{d}\Omega \\ D_{\theta\theta} &= \textstyle\int_\Omega c_v\,\mathrm{d}\Omega & D_{CC} &= \textstyle\int_\Omega h_v\,\mathrm{d}\Omega \end{aligned}$$

Minimizing Π_Ω in Eq. (27), we obtain the following linear system:

$$E\boldsymbol{X} = -D_{h\varepsilon}\Delta\bar{\epsilon}(t) - D_{h\theta}\Delta\theta(t) - D_{hC} \tag{28}$$

The fluctuation function $\boldsymbol{X}$ is linearly proportional to $\Delta\bar{\epsilon}(t)$ and $\Delta\theta(t)$, which means the solution can be written as

$$\boldsymbol{X} = \boldsymbol{\chi}_0\Delta\bar{\epsilon}(t) + \boldsymbol{\chi}_\theta\Delta\theta(t) + \boldsymbol{\chi}_C \tag{29}$$

Substituting Eq. (29) into Eq. (27), we can calculate the free energy density of the UC as

$$\Pi_\Omega = \frac{1}{2}[\Delta\bar{\epsilon}(t)]^T \mathrm{M}^*\Delta\bar{\epsilon}(t) + [\Delta\bar{\epsilon}(t)]^T\eta^*\Delta\theta(t) + [\Delta\bar{\epsilon}(t)]^T\varpi^* + \frac{1}{2}G^*\Delta\theta(t) + \frac{1}{2}c_v^*\frac{\Delta\theta(t)^2}{T_0} + \frac{1}{2}h_v^* \tag{30}$$

with

$$
\begin{aligned}
\mathrm{M}^* &= \frac{1}{\Omega}\left(\boldsymbol{\chi}_0^T D_{h\varepsilon} + D_{\varepsilon\varepsilon}\right)\\
\eta^* &= \frac{1}{\Omega}\left[\frac{1}{2}\left(D_{h\varepsilon}^T \boldsymbol{\chi}_\theta + \boldsymbol{\chi}_0^T D_{h\theta}\right) + D_{\varepsilon\theta}\right]\\
\varpi^* &= \frac{1}{\Omega}\left[\frac{1}{2}\left(D_{h\varepsilon}^T \boldsymbol{\chi}_C + \boldsymbol{\chi}_0^T D_{hC}\right) + D_{\varepsilon C}\right]\\
G^* &= \frac{1}{\Omega}\left[\boldsymbol{\chi}_C^T D_{h\theta} + \boldsymbol{\chi}_\theta^T D_{hC} + D_{\psi\psi}\right]\\
c_v^* &= \frac{1}{\Omega}\left(\boldsymbol{\chi}_\theta^T D_{h\theta} T_0 + D_{\theta\theta}\right)\\
h_v^* &= \frac{1}{\Omega}\left(\boldsymbol{\chi}_C^T D_{hC} + D_{CC}\right)
\end{aligned}
\tag{31}
$$

where M^* is a 6×6 material matrix condensed from the fourth-order instantaneous tensor $M_{ijkl}(t,\Psi)$; η^* is a 6×1 effective matrix containing the effective instantaneous second order thermal stress tensor η_{ij}^*; ϖ^* is a 6×1 effective matrix containing the effective instantaneous second order tensor ϖ_{ij}^*.

After having uniquely determined the fluctuation functions, we can recover the local displacement increments as

$$
\begin{Bmatrix} \Delta u_1(t)\\ \Delta u_2(t)\\ \Delta u_3(t)\end{Bmatrix} = \begin{Bmatrix} \Delta v_1(t)\\ \Delta v_2(t)\\ \Delta v_3(t)\end{Bmatrix} + \begin{bmatrix} \frac{\partial v_1}{\partial x_1} & \frac{\partial v_1}{\partial x_2} & \frac{\partial v_1}{\partial x_3}\\ \frac{\partial v_2}{\partial x_1} & \frac{\partial v_2}{\partial x_2} & \frac{\partial v_2}{\partial x_3}\\ \frac{\partial v_3}{\partial x_1} & \frac{\partial v_3}{\partial x_2} & \frac{\partial v_3}{\partial x_3}\end{bmatrix} \begin{Bmatrix} y_1\\ y_2\\ y_3\end{Bmatrix} + \bar{S}\hat{\boldsymbol{X}} \tag{32}
$$

where $\bar{S}$ is different from S and $\hat{\boldsymbol{X}}$ is different from $\boldsymbol{X}$ due to the recovery of slave nodes and the constrained node. The increments of the local strain field $\Delta\varepsilon(t)$ can be recovered as

$$
\Delta\varepsilon(t) = \Delta\bar{\varepsilon}(t) + \Gamma_h \bar{S}\hat{\boldsymbol{X}} \tag{33}
$$

where $\Delta\varepsilon(t) = \lfloor \Delta\varepsilon_{11}(t)\ 2\Delta\varepsilon_{12}(t)\ \Delta\varepsilon_{22}(t)\ 2\Delta\varepsilon_{13}(t)\ 2\Delta\varepsilon_{23}(t)\ \Delta\varepsilon_{33}(t)\rfloor^T$.

Finally, the increments of the local stress field can be recovered straightforwardly using the 3D constitutive relations for the constituent material as

$$
\Delta\sigma(t,\Psi) = M(t,\Psi)\Delta\varepsilon(t) + \eta(t,\Psi)\Delta\theta(t) + \varpi(t,\Psi) \tag{34}
$$

The simulations of the time-dependent and nonlinear behavior of SMA composites are performed using an incremental procedure based on Eq. (19). Once the M^*, η^*, and ϖ^* have been determined at the current loading, one can determine the current values of variables from previous values and increments according to

$$
\bar{\sigma}_{current} = \bar{\sigma}_{previous} + \Delta\bar{\sigma} \tag{35a}
$$

$$
\bar{\varepsilon}_{current} = \bar{\varepsilon}_{previous} + \Delta\bar{\varepsilon} \tag{35b}
$$

The simulations can be readily performed without applying various boundary conditions as those are carried out using finite element unit cell procedures.

4. Numerical examples

In this section, the proposed VAMUCH model was applied to characterize the effective time-dependent pseudoelastic behavior of SMA fiber reinforced polymer matrix composites in which the SMA fibers are of circular shape and in square array. Furthermore, $\Psi_{s0} = \Psi_{T0} = 0.0$ is assumed to be in all numerical examples. Since the effective pseudoelastic behavior is the strongest along the fiber direction, only longitudinal behavior was investigated in this study.

4.1. Material properties of SMA and polymer

SMA The material properties of SMA are presented in Table 1.

Polymer The polymer is assumed to be isotropic and linear thermoviscoelastic materials. The elastic relaxation modulus of the polymer can be expressed using Prony series as

$$
E(t) = E_0\left(1 - \sum_{k=1}^{n} g_k\left(1 - e^{-t/\tau_k}\right)\right) \tag{36}
$$

where E_0 is the instantaneous Young's modulus; g_k is dimensionless modulus and τ_k is the time relaxation material parameter. For simplicity, we considered a special case, namely, $n = 1$, $g_1 = 0.5$, and $\tau_1 = 30$, such that Eq. (36) is reduced to

$$
E(t) = 0.5E_0\left(1 + e^{-t/\rho}\right) = A + Be^{-t/\rho} \tag{37}
$$

Table 1
Thermomechanical material properties of Nitinol alloy Brinson, 1993.

Material properties	Transformation temperature	Model parameters
$E_A = 67000$ MPa	$M_f = 9.0\,^\circ$C	$C_M = 8.0$ MPa/$^\circ$C
$E_M = 26300$ MPa	$M_s = 18.4\,^\circ$C	$C_A = 13.8$ MPa/$^\circ$C
$\alpha_A = 11 \times 10^{-6}\,^\circ\text{C}^{-1}$	$A_s = 34.5\,^\circ$C	$\sigma_s^{Crit} = 100$ MPa
$\alpha_M = 6.6 \times 10^{-6}\,^\circ\text{C}^{-1}$	$A_f = 49.0\,^\circ$C	$\sigma_f^{Crit} = 170$ MPa
$\varepsilon^L = 0.067$		

where $E_0 = 8000$ MPa and $\rho = 30$, then $A = B = 4000$ MPa. The thermal expansion of the polymer material is kept constant as $\alpha = 54 \times 10^{-6}\,^\circ\text{C}^{-1}$.

The time-scale shift factor a_T in Eq. (3) is determined by empirical relationship of Williams–Landel–Ferry (WLF) (Williams, Landel, & Ferry, 1955),

$$\log a_T(T) = -\frac{C_1(T - T_0)}{C_2 + (T - T_0)} \tag{38}$$

where C_1 and C_2 are material constants determined through least squares fitting. In this example, the values of C_1 and C_2 are set as $C_1 = 4.92$ and $C_2 = 215.0$.

T_0 in Eq. (38) is the reference temperature and the temperature T at time t is given by

$$T = T_0 + \theta = T_0 + C_0 t \tag{39}$$

where C_0 is the temperature change rate.

Therefore, the reduced time $\xi(t + \Delta t)$, $\xi(t)$, and $\xi(\tau)$ are given by

$$\begin{aligned}
\xi(t + \Delta t) &= \int_0^{t+\Delta t} 10^{\frac{C_1 C_0 t'}{C_2 + C_0 t'}} \mathrm{d}t' \\
\xi(t) &= \int_0^{t} 10^{\frac{C_1 C_0 t'}{C_2 + C_0 t'}} \mathrm{d}t' \\
\xi(\tau) &= \int_0^{\tau} 10^{\frac{C_1 C_0 t'}{C_2 + C_0 t'}} \mathrm{d}t'
\end{aligned} \tag{40}$$

The stress relaxation stiffness matrix $[L_{ijkl}(t)]$ in Eq. (7) is obtained as

$$[L_{ijkl}(t)] = \mathrm{ff}[W] \tag{41}$$

where the coefficient ff is computed using Simpson's rule of numerical integration as

$$\mathrm{ff} = \frac{\Delta t}{6}(\mathrm{fL} + 4\mathrm{fm} + \mathrm{fu}) \tag{42}$$

where

$$\begin{aligned}
\mathrm{fL} &= A + Be^{-\frac{\xi(t+\Delta t) - \xi(t)}{\rho}} \\
\mathrm{fu} &= A + B \\
\mathrm{fm} &= A + Be^{-\frac{\xi(t+\Delta t) - \xi(t/2)}{\rho}}
\end{aligned}$$

The matrix $[W]$ in Eq. (41) is given by

$$[W] = \frac{1}{(1+\nu)(1-2\nu)} \begin{bmatrix}
1-\nu & \nu & \nu & 0 & 0 & 0 \\
\nu & 1-\nu & \nu & 0 & 0 & 0 \\
\nu & \nu & 1-\nu & 0 & 0 & 0 \\
0 & 0 & 0 & (1-2\nu)/2 & 0 & 0 \\
0 & 0 & 0 & 0 & (1-2\nu)/2 & 0 \\
0 & 0 & 0 & 0 & 0 & (1-2\nu)/2
\end{bmatrix} \tag{43}$$

with ν being the Poisson' ratio of the polymer, which is assumed to be constant $\nu = 0.4$.

The $\left[\gamma_{ij}(t)\right]$ is the matrix form of $\gamma_{ij}(t)$ in Eq. (7) and expressed as

$$\left[\gamma_{ij}(t)\right] = [L_{ijkl}(t)]\{\alpha\} \tag{44}$$

where $\{\alpha\}$ is a column matrix containing thermal expansion coefficients of the polymer materials.

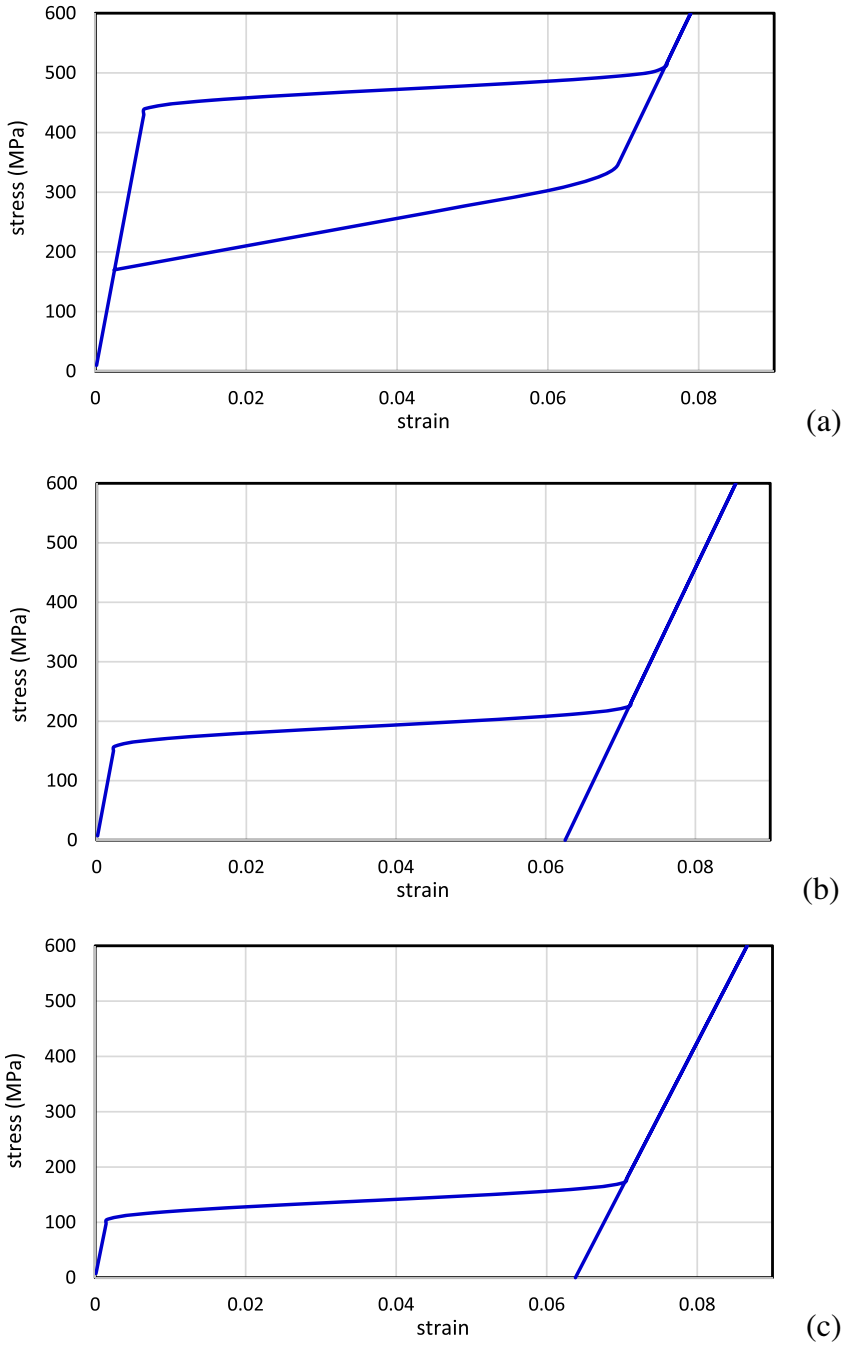

Fig. 2. Stress–strain curves of SMA in a loading–unloading loop calculated by VAMUCH at different temperatures: (a) $T = A_f + 11\ ^\circ\mathrm{C} = 60\ ^\circ\mathrm{C}$; (b) $T = M_s + 6.6\ ^\circ\mathrm{C} = 25\ ^\circ\mathrm{C}$; (c) $T = M_f + 6.0\ ^\circ\mathrm{C} = 15\ ^\circ\mathrm{C}$.

The coefficient matrix of $\omega_{ij}(t)$ in Eq. (7) is calculated as

$$\begin{aligned}\left[\omega_{ij}(t)\right] = \frac{B}{\Delta t}\sum_{i=1}^{n}\Bigg\{&\left(\int_{(i-1)\Delta t}^{i\Delta t}\left(e^{-(\xi(t+\Delta t)-\xi(\tau))/\rho} - e^{-(\xi(t)-\xi(\tau))/\rho}\right)[W]\mathrm{d}\tau\right)[\Delta\varepsilon(i)]\\ &+\left(\int_{(i-1)\Delta t}^{i\Delta t}\left(e^{-(\xi(t+\Delta t)-\xi(\tau))/\rho} - e^{-(\xi(t)-\xi(\tau))/\rho}\right)[W]\mathrm{d}\tau\right)\{\alpha\}\Delta\theta(i)\Bigg\}\end{aligned} \tag{45}$$

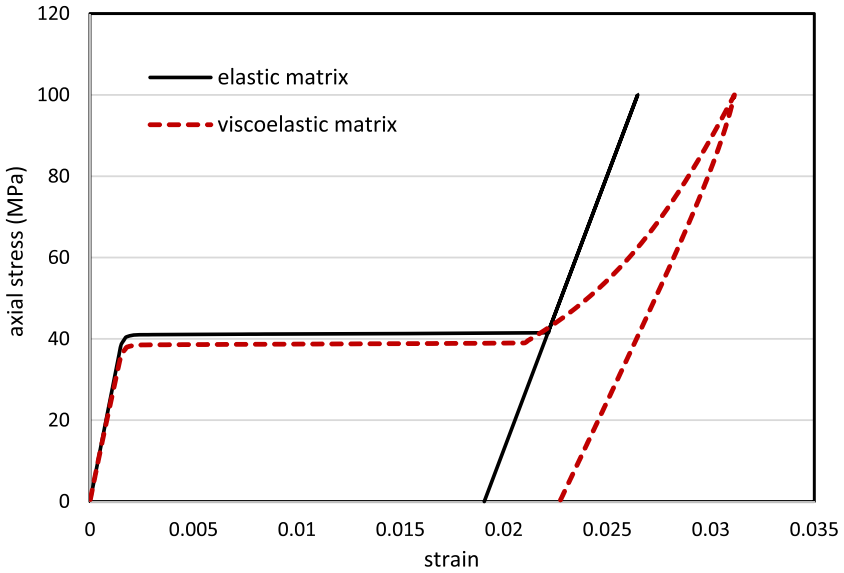

Fig. 3. Axial stress–strain curves ($\bar{\sigma}_{11}$ vs $\bar{\varepsilon}_{11}$) of SMA composites (vof $= 0.3$) with viscoelastic polymer matrix and elastic matrix, respectively, at temperature $T = M_f + 6.0\,^{\circ}\mathrm{C} = 15\,^{\circ}\mathrm{C}$, where the Young's modulus of the elastic matrix has the same value as the instantaneous Young's modulus of polymer.

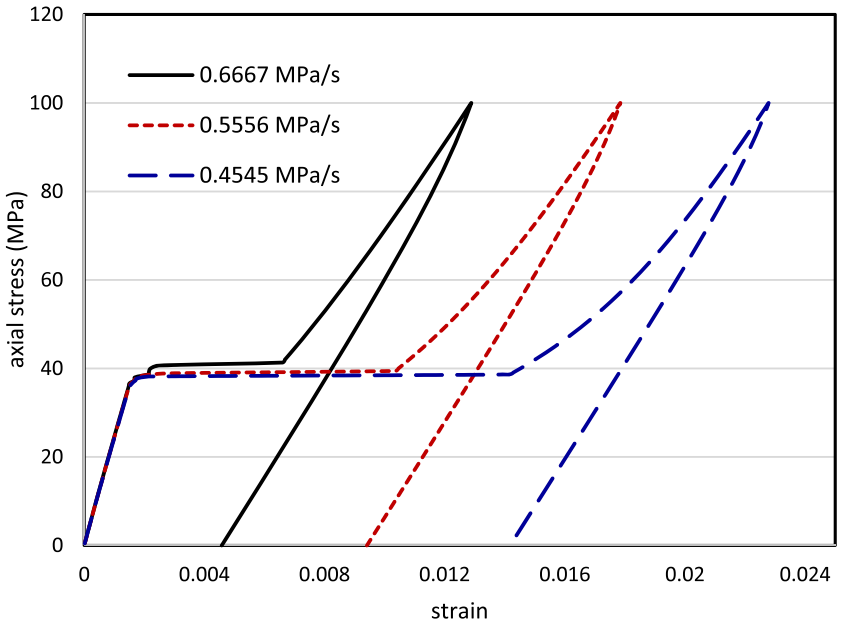

Fig. 4. Predicted axial stress–strain curves ($\bar{\sigma}_{11}$ vs $\bar{\varepsilon}_{11}$) of SMA polymer matrix composites (vof $= 0.3$) in a loading–unloading loop at different loading rates when the temperature is $T = M_f + 6.0\,^{\circ}\mathrm{C} = 15\,^{\circ}\mathrm{C}$.

where $[\Delta\varepsilon(i)]$ is 6×1 column matrix containing strain increments during the ith time step Δt; $\Delta\theta(i)$ is the increment of temperature change during the ith time step Δt; and $n = t/\Delta t$.

4.2. Simulation results and discussions

Firstly, the stress–strain curves of pure SMA at various temperatures in a loading–unloading loop were calculated by VAMUCH and shown in Fig. 2. One can observe that the stress-induced martensitic transformation start when the stress values reach critical values and after that the material responses soften due to the large transformation strain. The responses of SMA before the end of martensitic transformation during loading are similar to bilinear hardening plastic deformation. After

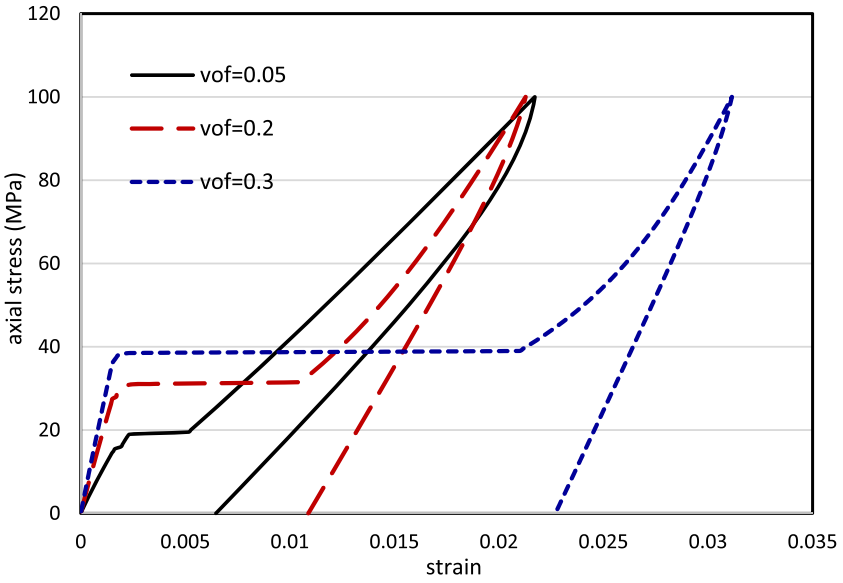

Fig. 5. Predicted axial stress–strain curves ($\bar{\sigma}_{11}$ vs $\bar{\varepsilon}_{11}$) of SMA polymer matrix composites in a loading–unloading loop at various volume fractions of the SMA fibers, eg., vof = 0.05, 0.2, and 0.3 when the temperature is $T = M_f + 6.0\,^{\circ}\mathrm{C} = 15\,^{\circ}\mathrm{C}$.

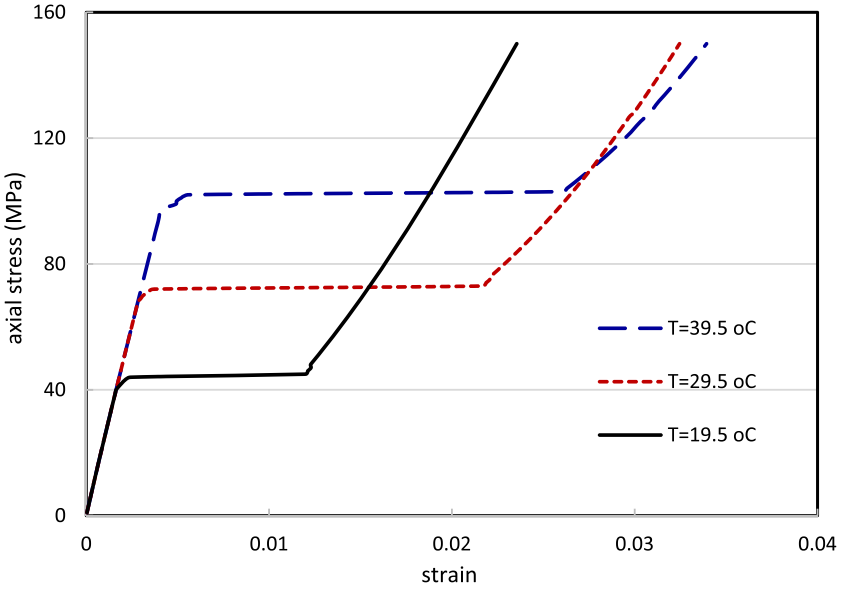

Fig. 6. Predicted axial stress–strain curves ($\bar{\sigma}_{11}$ vs $\bar{\varepsilon}_{11}$) of SMA polymer matrix composites (vof = 0.3) on loading at various temperatures $T = 39.5\,^{\circ}\mathrm{C}$,29.5 °C, and 19.5 °C.

the martensitic transformation finishes, the material becomes pure elastic martensite. When the temperature is higher than A_s, see Fig. 2(a), the reverse transformation (from martensite to austenite) occurs once the stress values are lower than the critical values during unloading. After the reverse transformation finishes, the material recovers to pure elastic austenite. If the temperature is lower than A_s, see Fig. 2(b) and (c), no reverse transformation happens and large permanent deformation occurs after unloading.

Fig. 3 shows the axial stress–strain curves of SMA fiber composites with viscoelastic polymer matrix and elastic matrix, respectively, where the Young's modulus of the elastic matrix has the same value as the instantaneous Young's modulus of polymer, $E_0 = 8000$ MPa. The volume fraction of the SMA fiber is vof = 0.3. It is obviously observed that the loading and unloading paths of viscoelastic polymer matrix composites do not coincide but form a hysteresis loop, which is apparently different from the response of elastic matrix composite. Stemming from the viscoelastic behavior of polymer matrix, the

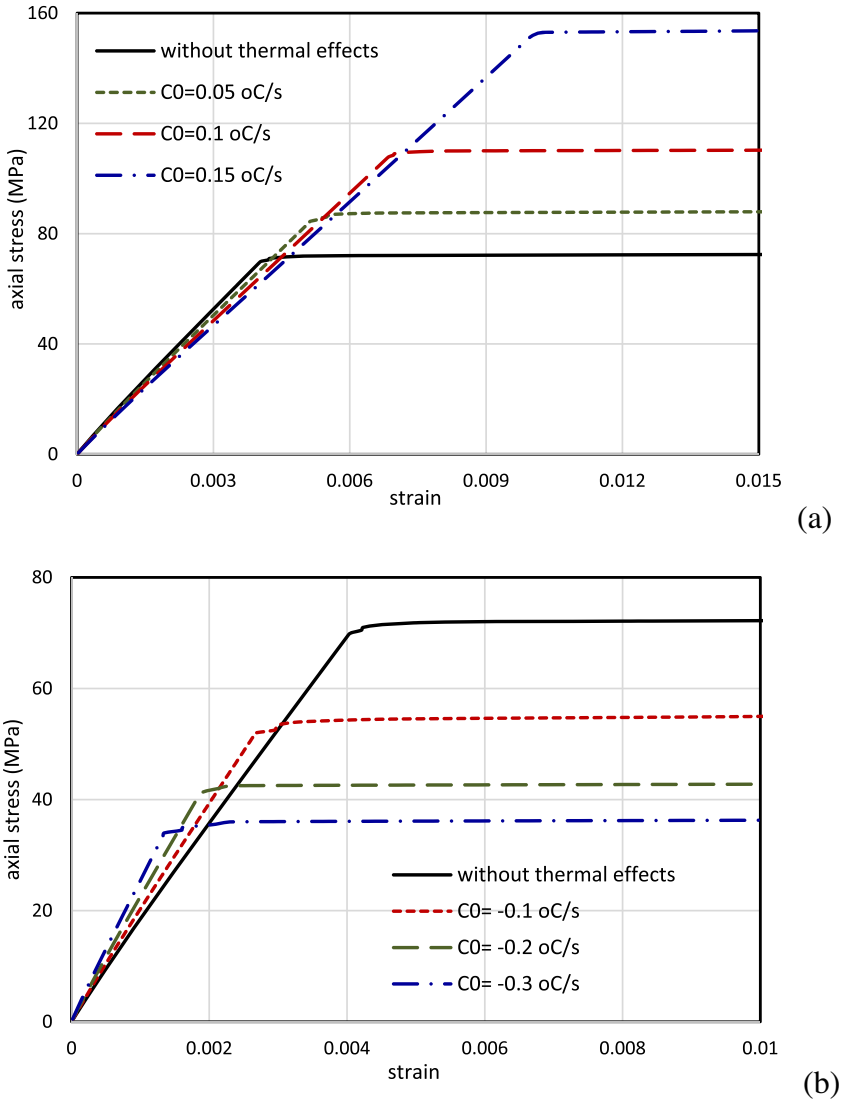

Fig. 7. The influences of temperature change rates on the effective viscoelastic stiffness and critical stress of macroscopic martensitic transformation of SMA polymer matrix composites (vof $= 0.2$): (a) positive temperature change rate, $C_0 = 0.05$, 0.1, and 0.15 °C/s; (b) negative temperature change rate, $C_0 = -0.1$, -0.2, and -0.3 °C/s. The initial temperature is $T = A_s + 5.0$ °C $= 39.5$ °C and the mechanical loading rate is kept constant as 0.5 MPa/s.

stress–strain curves of polymer matrix composites are strongly dependent on the loading rates. Fig. 4 illustrates the predicted axial stress–strain curves ($\bar{\sigma}_{11}$ vs $\bar{\varepsilon}_{11}$) of SMA polymer matrix composites (vof $= 0.3$) in a loading–unloading loop at different loading rates when the temperature is $T = M_f + 6.0$ °C $= 15$ °C. The responses of the composite become stronger with the increase of the loading rates, which means that the faster the loading the higher the critical stress of macroscopic transformation.

Fig. 5 demonstrates the predicted axial stress–strain curves ($\bar{\sigma}_{11}$ vs $\bar{\varepsilon}_{11}$) of SMA polymer matrix composites in a loading–unloading loop at various volume fractions of the SMA fibers, e.g., vof $= 0.05, 0.2,$ and 0.3 when the temperature is $T = M_f + 6.0$ °C $= 15$ °C. It is evident that the total deformation, the effective viscoelastic stiffness, and critical stress of macroscopic martensitic transformation increase with the increase of the volume fractions of SMA fibers.

In order to investigate the influences of temperature, the effective axial stress–strain curves of SMA polymer matrix composites on loading were calculated at various temperatures $T = 39.5$ °C, 29.5 °C, and 19.5 °C and plotted in Fig. 6. The critical stress of macroscopic martensitic transformation increase with the increase of the temperature since the critical stress of martensitic transformation of pure SMA is higher at higher temperature as illustrated in Fig. 2.

Finally, the influences of temperature change rates on the effective viscoelastic stiffness and critical stress of macroscopic martensitic transformation of SMA polymer matrix composites (vof $= 0.2$) on loading were calculated with: (a) positive temperature change rate, $C_0 = 0.05$, 0.1, and 0.15 °C/s; and (b) negative temperature change rate, $C_0 = -0.1$, -0.2, and

$-0.3\ ^{\circ}\mathrm{C/s}$, respectively. The initial temperature is $= A_s + 5.0\ ^{\circ}\mathrm{C} = 39.5\ ^{\circ}\mathrm{C}$. The mechanical loading rate is kept constant as 0.5 MPa/s and applied simultaneously with thermal loading. From Fig. 7(a) one can observe that the effective viscoelastic stiffness decreased but the critical stress of macroscopic martensitic transformation increased as the absolute values of positive temperature change rates increased. This is because the composite's response is the combined responses of its constituents. The critical stress of martensitic transformation of SMA increases with temperature increasing but the thermal expansion of both constituents with the increase of temperature cause the softening response of the composites. Hence, the influences of the absolute values of the negative temperature change rates, see Fig. 7(b), are opposite.

5. Conclusions

Based on the theoretical framework of VAMUCH, a micromechanical model that is capable of determining the macroscopic time-dependent and nonlinear pseudoelastic response of composites composed of polymer matrix and SMA has been developed. The derivation of the proposed model starts from the variational statement of an energy functional generated from the unified formulation for both polymer and SMA. Due to the time-dependent characteristics and nonlinearity of the composite, the present model was developed by adopting an incremental procedure associated with instantaneous tangential matrices. Although the numerical studies were performed on SMA fiber composites, the present model can be readily applied to composites with arbitrary number and geometry of SMA reinforcements. The numerical results clearly demonstrated that the viscoelasticity of polymer matrix significantly induced the viscoelastic behavior of composites, namely, rate-dependent behavior and hysteresis behavior. Despite the pseudoelastic responses are focus of this study, the present model is a general purpose tool which can be easily extended to model shape memory effect and the effects of viscoplastic matrix.

References

Aboudi, J. (1996). Micromechanical analysis of composites by the method of cells – Update. *Applied Mechanics Reviews, 49*, S83–S91.

Aboudi, J. (2004). The generalized method of cells and high-fidelity generalized method of cells micromechanical models – A review. *Mechanics of Advanced Materials and Structures, 11*(4-5), 329–366.

Achenbach, M., & Müller, I. A. (1982). A model for shape memory. *Journal de Physique, 12*(43), 163–167.

Birman, V. (1997). Review of mechanics of shape memory alloy structures. *Applied Mechanics Reviews, 50*, 629–645.

Birman, V., Saravanos, D. A., & Hopkins, D. A. (1996). Micromechanics of composites with shape memory alloy fibers in uniform thermal fields. *AIAA Journal, 34*(9), 1905–1912.

Bodner, S. R. (2002). *Unified plasticity for engineering applications*. New York: Kluwer.

Boyd, J. G., & Lagoudas, D. C. (1994). Thermomechanical response of shape memory composites. *Journal of Intelligent Material Systems and Structures, 5*, 333–346.

Brinson, L. C. (1993). One-dimensional constitutive behavior of shape memory alloys: Thermomechanical derivation with non-constant material functions and redefined martensite internal variable. *Journal of Intelligent Material Systems and Structures, 4*, 229–242.

Brinson, L. C., & Lammering, R. (1993). Finite element analysis of the behavior of shape memory alloys and their applications. *International Journal of Solids and Structures, 30*, 3261–3280.

Chamis, C.C. (1983). Simplified composite micromechanics equation for hygral, thermal and mechanical properties. NASATM-83320.

Damanpack, A. R., Aghdam, M. M., & Shakeri, M. (2015). Micro-mechanics of composite with SMA fibers embedded in metallic/polymeric matrix under off-axial loadings. *European Journal of Mechanics – A/Solids, 49*, 467–480.

Freed, Y., & Aboudi, J. (2009). Thermomechanically coupled micromechanical analysis of shape memory alloy composites undergoing transformation induced plasticity. *Journal of Intelligent Material Systems and Structures, 20*(23), 23–38.

Gilat, R., & Aboudi, J. (2004). Dynamic response of active composite plates: Shape memory alloy fibers in polymeric/metallic matrices. *International Journal of Solids and Structures, 41*, 5717–5731.

Jani, J. M., Leary, M., Subic, A., & Gibson, M. A. (2014). A review of shape memory alloy research, applications and opportunities. *Materials and Design, 56*, 1078–1113.

Jarali, C. S., Raja, S., & Upadhya, A. R. (2008). Micro-mechanical behaviors of SMA composite materials under hygro-thermo-elastic strain fields. *International Journal of Solids and Structures, 45*, 2399–2419.

Lagoudas, D. C. (2008). *Shape memory alloys: Modeling and engineering applications*. Springer.

Lagoudas, D. C., BO, Z., & Qidwai, M. A. (1996). A unified thermodynamic constitutive model for SMA and finite element analysis of active metal matrix composites. *Mechanics of Composite Materials and Structures, 3*, 153–179.

Mura, T. (1982). *Micromechanics of defects in solids*. Martinus Nijhoff Publishers.

Nishiyama, Z. (1978). *Martensitic transformation*. New York: Academic Press.

Paiva, A., & Savi, M. A. (2006). An overview of constitutive models for shape memory alloys. *Mathematical Problems in Engineering, 2006*, 1–30.

Paiva, A., Savi, M. A., Braga, A. M. B., & Pacheco, P. M. C. L. (2005). A constitutive model for shape memory alloys considering tensile-compressive asymmetry and plasticity. *International Journal of Solids and Structures, 42*, 3439–3457.

Panico, M., & Brinson, L. (2007). A three-dimensional phenomenological model for martensite reorientation in shape memory alloys. *Journal of the Mechanics and Physics of Solids, 55*, 2491–2511.

Panico, M., & Brinson, L. (2007). A three-dimensional phenomenological model for martensite reorientation in shape memory alloys. *Journal of the Mechanics and Physics of Solids, 55*, 2491–2511.

Perkins, J. (1975). *Shape memory effects in alloys*. New York: Plenum Press.

Pyatigorets, A. V., Marasteanu, M. O., Khazanovich, L., & Stolarski, H. K. (2010). Application of a matrix operator method to the thermocviscoelastic analysis of composite structures. *Journal of Mechanics of Materials and Structures, 5*(5), 837–854.

Saravanos, D. A., Birman, V., & Hopkins, D. A. (1995). Micromechanics and stress analysis of composites with shape memory alloy fibers in uniform thermal fields. *AIAA Journal*, 433–443.

Tang, T., & Felicelli, D. S. (2015) A micromechanical model for hygrothermoelastic heterogeneous materials. In *Proceedings of TMS 2015 144th annual meeting & exhibition*, Orlando, Florida.

Warlimont, H., Delaey, L., Krishnan, R. V., & Tas, H. (1974). Thermoelasticity, pseudoelasticity and the memory effects associated with martensitic transformations – Part 3: Thermodynamics and kinetics. *Journal of Materials Science, 9*(9), 1545–1555.

Williams, M. L., Landel, R. F., & Ferry, J. D. (1955). The temperature dependence of relaxation mechanisms in amorphous polymers and other glass-forming liquids. *Journal of the American Chemical Society, 77*(14), 3701–3707.

Wineman, A. S., & Rajagopal, K. R. (2000). *Mechanical response of polymers: An introduction*. New York: Cambridge University Press.
Yu, W., & Tang, T. (2007). Variational asymptotic method for unit cell homogenization of periodically heterogeneous materials. *International Journal of Solids and Structures, 44*, 3738–3755.
Yu, W., & Tang, T. (2007). A variational asymptotic micromechanics model for predicting thermoelastic properties of heterogeneous materials. *International Journal of Solids and Structures, 44*(22-23), 7510–7525.